Progress In Electromagnetics Research M, Vol. 102, 171–180, 2021

Modern Applications of the Bateman-Whittaker Theory

Ioannis M. Besieris[1, *], Peeter Saari[2, 3], and Amr M. Shaarawi[4]

Abstract—The Bateman-Whittaker theory, which was developed a century ago, is shown to be a comprehensive basis for deriving a large class of null spatiotemporally localized electromagnetic waves characterized by intriguing vortical structures. In addition, it provides the modeling for studying topological structures dealing with linked and knotted electromagnetic waves.

1. INTRODUCTION

Electromagnetic waves are most conveniently expressed in terms of a complex-valued vector, first introduced by Riemann [1] and afterwards by Silberstein [2]. Let $\vec{E}(\vec{r},t)$ and $\vec{B}(\vec{r},t)$ denote, respectively, the *real-valued* electric and magnetic fields satisfying the homogeneous Maxwell equations in *free* space. Then, the Riemann-Silberstein vector in SI units is defined as follows:

$$\vec{F} = \sqrt{\frac{\varepsilon_0}{2}} \left(\vec{E} + ic\vec{B} \right). \tag{1}$$

It obeys the equations

$$\nabla \times \vec{F} = i\frac{1}{c}\frac{\partial}{\partial t}\vec{F}, \quad \nabla \cdot \vec{F} = 0, \tag{2}$$

which are exactly equivalent to the original Maxwell equations for the real fields.

Several important physical quantities associated with the real fields can be expressed conveniently in terms of $\vec{F}(\vec{r},t)$. Specifically, the Poynting vector, electromagnetic field energy density, electromagnetic momentum density, and electromagnetic angular momentum density can be written as

$$\begin{aligned} \vec{P} &= \vec{E} \times \vec{H} = -ic\vec{F}^* \times \vec{F}, \\ w_{em} &= \frac{1}{2}\left(\varepsilon_0 \vec{E}\cdot\vec{E} + \mu_0 \vec{H}\cdot\vec{H}\right) = \vec{F}\cdot\vec{F}^*, \\ \vec{M} &= \frac{1}{c^2}\vec{E}\times\vec{H} = -i\frac{1}{c}\vec{F}^*\times\vec{F}, \\ \vec{J} &= \vec{r}\times\vec{M} = -i\frac{1}{c}\vec{r}\times\left(\vec{F}^*\times\vec{F}\right), \end{aligned} \tag{3}$$

respectively.

Using a variation of the Hertz vector potential approach, a general solution to Eq. (2) can be written as follows [3]:

$$\begin{aligned} \vec{F}(\vec{r},t) &= \nabla\times\nabla\times\vec{\Pi} + \frac{i}{c}\frac{\partial}{\partial t}\nabla\times\vec{\Pi}; \\ \vec{\Pi}(\vec{r},t) &= \vec{a}\,\psi(\vec{r},t). \end{aligned} \tag{4}$$

Received 8 April 2021, Accepted 14 May 2021, Scheduled 19 May 2021

* Corresponding author: Ioannis M. Besieris (besieris@vt.edu).
[1] The Bradley Department of Electrical and Computer Engineering, Virginia Polytechnic Institute and State University, Blacksburg VA 24060, USA. [2] Institute of Physics, University of Tartu, W. Ostwaldi 1, Tartu 50411, Estonia. [3] Estonian Academy of Sciences, Kohtu 6, 10130, Tallinn, Estonia. [4] Department of Physics, The American University of Cairo, P.O. Box 74, New Cairo 11835, Egypt.

Here, $\vec{a}$ is a constant vector, and $\psi(\vec{r},t)$ is a complex-valued solution to the homogeneous scalar wave equation.

2. BATEMAN-WHITTAKER THEORY

Possibly motivated by Whittaker's two-scalar potential theory [4], Bateman [5] introduced two complex-valued scalar functions $\alpha(\vec{r},t)$ and $\beta(\vec{r},t)$, known as the *Bateman conjugate functions*, so that an arbitrary functional $\phi[\alpha(\vec{r},t),\beta(\vec{r},t)]$ obeys the nonlinear characteristic (eikonal) equation

$$\left(\frac{\partial\phi}{\partial x}\right)^2+\left(\frac{\partial\phi}{\partial y}\right)^2+\left(\frac{\partial\phi}{\partial z}\right)^2-\frac{1}{c^2}\left(\frac{\partial\phi}{\partial t}\right)^2=0. \tag{5}$$

Furthermore, two functionals $\phi_{1,2}[\alpha(\vec{r},t),\beta(\vec{r},t)]$ obey the *Bateman constraint relation*

$$\nabla\phi_1\times\nabla\phi_2=i\frac{1}{c}\left(\frac{\partial\phi_1}{\partial t}\nabla\phi_2-\frac{\partial\phi_2}{\partial t}\nabla\phi_1\right). \tag{6}$$

Next, the Riemann-Silberstein vector is defined as

$$\vec{F}=\sqrt{\frac{\varepsilon_0}{2}}\left(\vec{E}+ic\vec{B}\right)=\sqrt{\frac{\varepsilon_0}{2}}c\nabla\times\vec{A}=\sqrt{\frac{\varepsilon_0}{2}}c\alpha^{p-1}\beta^{q-1}\nabla\alpha\times\nabla\beta, \tag{7}$$

in terms of the complex-valued vector potential $\vec{A}=(\varepsilon_0/2)^{1/2}c(pq)^{-1}\alpha^p\nabla\beta^q=\vec{A}_e+i\vec{A}_m$, where $p,q=0,1,2,3,\ldots$. By virtue of its construction, the Riemann-Silberstein vector in Eq. (7) obeys Eq. (2). Therefore, $\vec{E}=(1/c)\nabla\times\vec{A}_e$ and $\vec{B}=\nabla\times\vec{A}_m$. The real electric and magnetic vector potentials can be used to determine the total electric and magnetic helicities, viz.,

$$h_e=\int_{R^3}d\vec{r}\vec{A}_e\cdot\vec{E},\quad h_m=\int_{R^3}d\vec{r}\vec{A}_m\cdot\vec{B}. \tag{8}$$

Another consequence of the specific construction of the Riemann-Silberstein vector is the nullity property:

$$\begin{aligned}&\vec{F}(\vec{r},t)\cdot\vec{F}(\vec{r},t)=i\varepsilon_0 I_2+\frac{\varepsilon_0}{2}I_1=0;\\&I_1=\left|\vec{E}(\vec{r},t)\right|^2-c^2\left|\vec{B}(\vec{r},t)\right|^2=0,\\&I_2=\vec{E}(\vec{r},t)\cdot\vec{B}(\vec{r},t)=0.\end{aligned} \tag{9}$$

It requires, specifically, that the two relativistic invariants $I_{1,2}$ vanish identically. The corresponding real fields $\vec{E}(\vec{r},t)$ and $\vec{B}(\vec{r},t)$ are called *null electromagnetic fields*. Such fields are transverse with respect to the local flow of energy, which is equipartitioned between the electric and magnetic fields, and the *modulus of their local energy transport velocity equals the speed of light in vacuo*, although this velocity can vary both spatially and temporally. The simplest electromagnetic null field is a plane wave. More complex null fields are characterized by "helical" or vortex structures on planes transverse to the direction of propagation and, in general, are relatively simple so that explicit calculations can be made of the total energy and the total angular momentum they carry.

3. MOTIVATION FOR THE BATEMAN CONJUGATE FUNCTIONS

Courant and Hilbert have pointed out that "relatively undistorted" progressive solutions to the homogeneous scalar wave equation in free space assume the form $\psi(\vec{r},t)=g(\vec{r},t)f[\theta(\vec{r},t)]$, where $f(\cdot)$ is essentially an arbitrary function; $\theta(\vec{r},t)$, referred to as the "phase" function, is a solution to the nonlinear characteristic equation [cf. Eq. (5)]; $g(\vec{r},t)$ is an "attenuation" function; the latter depends on the choice of $\theta(\vec{r},t)$, but not in a unique manner.

The nonlinear characteristic equation has an infinite number of phase solutions $\theta(\vec{r},t)$. Once a solution has been found, one introduces the Courant-Hilbert *ansatz* into the wave equation in order to determine the accompanying attenuation function $g(\vec{r},t)$. Although straightforward, this procedure is usually laborious. Recently, efficient and encompassing methods for realizing attenuation and phase functions have been developed in connection with the derivation of spatiotemporally localized waves [6]. Such wave pulses exhibit distinct advantages in their performance in comparison to conventional quasi-monochromatic signals. It has been shown that such wavepackets have extended ranges of localization in the near-to-far field regions. Among the localized waves, the subclass of solutions conforming to the Courant-Hilbert *ansatz* yields indirectly specific realizations of the attenuation function $g(\vec{r},t)$ and the phase function $\theta(\vec{r},t)$.

4. SPATIOTEMPORALLY LOCALIZED WAVES

A very general class of *luminal* localized solutions to the homogeneous scalar wave equation is given by

$$\begin{aligned} \psi_L(\vec{r},t) &= g_L(\vec{r},t)\, f\left[\theta\left(\alpha_L,\beta_L\right)\right]; \\ g_L(\vec{r},t) &= \frac{1}{a_1 + i\,(z-ct)}, \\ \alpha_L(\vec{r},t) &= a_2 - i\,(z+ct) + \frac{x^2+y^2}{a_1+i\,(z-ct)}. \\ \beta_L(\vec{r},t) &= \frac{x-iy}{a_1+i\,(z-ct)}, \end{aligned} \tag{10}$$

where $z \pm ct$ are the characteristic variables of the one-dimensional scalar wave equation, and $a_{1,2}$ are positive free parameters. The functions $\alpha_L(\vec{r},t)$ and $\beta_L(\vec{r},t)$ are, indeed, Bateman conjugate functions obeying the nonlinear characteristic equation, as well as the Bateman constraint. Therefore, they can be used in conjunction to Eq. (7) to derive luminal null electromagnetic field solutions to Maxwell's equations.

As a specific example of a scalar luminal spatiotemporally localized wave, the finite-energy azimuthally symmetric modified power spectrum (MPS) pulse, derived originally by Ziolkowski [7], follows from the choice

$$f\left[\alpha_L(\vec{r},t)\right] = \exp\left[-\left(b/p\right)\alpha_L(\vec{r},t)\right]\left(a_2 + \alpha_L(\vec{r},t)/p\right)^{-q}$$

in Eq. (10). Here, $a_2,\ b,\ p$, and q are free positive parameters. For

$$f\left[\alpha_L(\vec{r},t),\beta_L(\vec{r},t)\right] = \left[a_2 + \alpha_L(\vec{r},t)\right]^{-q}\beta_L^m(\vec{r},t),$$

with $a_2,\ q > 0$ and m a nonnegative integer, one obtains the asymmetric version of Ziolkowski's scalar splash wave mode. For $m = 0$, this solution follows from the MPS pulse under the restrictions $b = 0,\ p = 1$. Finally, for $b = p = \beta,\ a_2 = 0$ and $q = 0$, it reduces to the infinite-energy focus wave mode (FWM).

It should be emphasized that only the conjugate functions $\alpha_L(\vec{r},t)$ and $\beta_L(\vec{r},t)$ enter into the computation of the luminal null localized electromagnetic fields based on the Bateman-Whittaker theory. The attenuation function plays no role. However, it is needed if the luminal scalar wave function in Eq. (10) is used in conjunction to Eq. (4) to compute the Riemann-Silberstein complex vector. Although the latter will obey Eqs. (2a) and (2b), it will not be null unless the vector $\vec{a}$ in Eq. (4) is chosen appropriately.

Analogous to Eq. (10), there exist expressions for subluminal and superluminal localized scalar wave solutions, with corresponding Bateman conjugate functions.

A general class of *superluminal* localized solutions to the homogeneous scalar wave equation in free space is given by

$$\begin{aligned} \psi_S(\vec{r},t) &= g_S(\vec{r},t)\, f\left[\theta\left(\alpha_S,\beta_s\right)\right]; \\ g_S(\vec{r},t) &= \frac{1}{\sqrt{x^2+y^2+\left(a_1+i\gamma\varsigma\right)^2}}, \\ \alpha_S(\vec{r},t) &= a_2 - i\gamma\,(v/c)\,\eta + \sqrt{x^2+y^2+\left(a_1+i\gamma\varsigma\right)^2}. \\ \beta_S(\vec{r},t) &= \frac{x-iy}{a_1+i\gamma\varsigma+\sqrt{x^2+y^2+\left(a_1+i\gamma\varsigma\right)^2}}. \end{aligned} \tag{11}$$

Here, $\varsigma = z - vt,\ \eta = z - (c^2/v)t,\ \gamma = ((v/c)^2 - 1)^{-1/2}$, with $v > c$.

A particular example follows from the complex analytic signal

$$f\left[\alpha_S\right] = \exp\left[-\left(b/p\right)\alpha_S\right]\left[a_2 + \left(1/p\right)\alpha_S\right]^{-q},$$

where a_2, b, and q are positive real parameters. The resulting solution is the finite-energy modified focus X wave (MFXW) pulse derived by Besieris *et al.* [6] if $p = 1$.

It should be noted that both the general classes of luminal and superluminal localized waves given in Eqs. (10) and (11), respectively, are characterized by two speeds. The first class is bidirectional involving the characteristic variables $z \pm ct$ of the one-dimensional scalar wave equation. The latter involves the superluminal speed v, as well as the subluminal speed c^2/v.

A general class of *unidirectional* (along the z-direction) spatiotemporally localized waves in free space is given by

$$\begin{aligned}
\psi_U\left(\vec{r},t\right) &= g_U\left(x,y,t\right) f\left[\theta\left(\alpha_U,\beta_U\right)\right];\\
g_U\left(\rho,t\right) &= \frac{1}{\sqrt{x^2+y^2-\left[ct+i\left(a_1+a_2\right)/2\right]^2}},\\
\alpha_U\left(\vec{r},t\right) &= i\,z + \left(a_1-a_2\right)/2 + \sqrt{x^2+y^2-\left[ct+i\left(a_1+a_2\right)/2\right]^2},\\
\beta_U\left(x,y,t\right) &= \frac{x+iy}{-ict+\left(a_1+a_2\right)/2+\sqrt{x^2+y^2-\left[ct+i\left(a_1+a_2\right)/2\right]^2}},
\end{aligned} \tag{12}$$

where the free parameters $a_{1,2}$ are positive. This class of solutions significantly extends the simple unidirectional finite-energy pulse introduced by So *et al.* [8] recently.

5. NULL SPATIOTEMPORALLY LOCALIZED WAVES

The Riemann-Silberstein vector defined in Eq. (7) is null for any values of p and q. Specifically, for $p = 1$ and $q = 1$, the null vector $\vec{F}^{(f)} = \nabla\alpha \times \nabla\beta$ will be called the *fundamental Riemann-Silberstein vector*. The product of this expression with any functional of α and β results in a null Riemann-Silberstein vector.

A general formula for constructing null luminal, superluminal, and unidirectional spatiotemporally localized waves is as follows:

$$\begin{aligned}
\vec{F}_{L,S,U} &= g^{-1}_{L,S,U}\left(\vec{r},t\right)\psi_{L,S,U}\left(\vec{r},t\right)\vec{F}^{(f)}_{L,S,U};\\
\vec{F}^{(f)}_{L,S,U} &= \nabla\alpha_{L,S,U} \times \nabla\beta_{L,S,U};\\
\vec{E}_{L,S,U} &= \sqrt{\frac{2}{\varepsilon_0}}\mathrm{Re}\left\{\vec{F}_{L,S,U}\right\}, \quad \vec{H}_{L,S,U} = \sqrt{\frac{2}{\mu_0}}\mathrm{Im}\left\{\vec{F}_{L,S,U}\right\}.
\end{aligned} \tag{13}$$

Here, the indices L, S, U stand for luminal, superluminal, and unidirectional, respectively. It should be noted that the attenuation factors $g_{L,S,U}(\vec{r},t)$ do not enter the derivation because $\psi_{L,S,U}\,g^{-1}_{L,S,U}(\vec{r},t) = Q[\alpha_{L,S,U}(\vec{r},t), \beta_{L,S,U}(\vec{r},t)]$. This is consistent with Eq. (7).

Examples of null luminal and superluminal localized waves have been given in Refs. [9] and [10]. A specific example of a null unidirectional electromagnetic localized wave results from the algorithm in Eq. (13) with

$$\psi_U\left(\vec{r},t\right) = \frac{1}{\sqrt{x^2+y^2-\left[ct+i\left(a_1+a_2\right)/2\right]}}\frac{1}{\alpha_U^3}\beta_U^{n-1}. \tag{14}$$

This is equivalent to deriving the Riemann-Silberstein vector $\vec{F}_U(\vec{r},t)$ using the expression in Eq. (7) with $\alpha = \alpha_U^{-2},\ \beta = \beta_U^n/(2n)$ and $p = q = 1$.

The group speed of the unidirectional pulse in Eq. (14), and as a consequence of the corresponding null electromagnetic localized wave, is given by

$$v_g\left(\rho,t\right) = c\,\mathrm{Re}\left\{\frac{\left(a_1+a_2\right)/2 - ict}{\sqrt{\left[\left(a_1+a_2\right)/2 - ict\right]^2 + \rho^2}}\right\}, \tag{15}$$

where $\rho = \sqrt{x^2 + y^2}$ is the radial distance in cylindrical coordinates. It is seen that the group speed depends on both the radial distance and time. A plot of the group speed (normalized with respect to the speed of light in vacuum equal to unity) is shown in Figure 1 below for various values of ρ. On axis ($\rho = 0$), $v_g = 1$ for all values of time. At $\rho = 2$, the speed is subluminal (but very close to unity) for small values of time, and it becomes luminal at $t = 5$, superluminal (again, very close to unity) for $t > 5$ and tends to unity for large values of time. A similar behavior is exhibited for larger values of ρ.

A few additional graphical results will be presented to gain a clearer view of some of the features of the null unidirectional electromagnetic localized wave. The following notation will be used next: $\varsigma \equiv z - ct$ is the local spatial coordinate around the pulse center; therefore, ct is the distance from the "aperture" located at $z = 0$. For all the figures, the parameter values are as follows: $a_1 = 10^{-6}m$ and $a_2 = 10^{-3}m$. On the top row of Fig. 2, plots of $|E_x|$ vs. $\bar{\varsigma} = \varsigma/a_1$ and $\bar{\rho} = \rho/(10a_1)$ are shown on the aperture plane ($ct = 0$) and on the planes $ct = \pm 4 \times 10^{-4}m$. Similar plots are shown on the second row for $|E_z|$.

On the top row of Fig. 3, plots of $|E_x|$ vs. $\bar{x} = x/(10^2 a_1)$ and $\bar{y} = y/(10^2 a_1)$ are shown at $\tau \equiv t - z/c = 0$ and $\tau = \pm 10^{-6}s$. Similar plots are shown on the second row for $|E_z|$. An antisymmetric "helical" structure to the left and right of the pulse center is clearly evident.

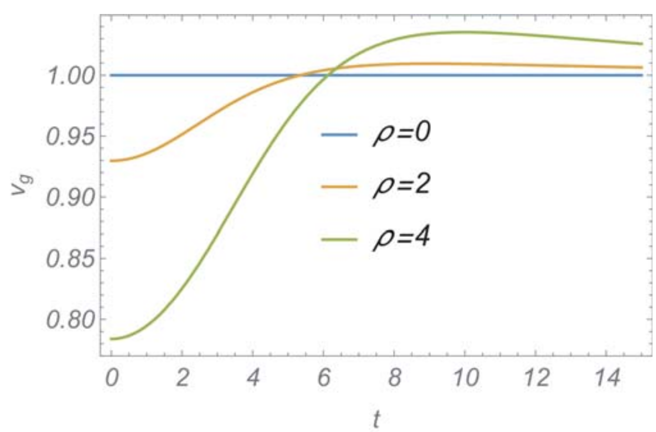

Figure 1. Plot of the normalized group speed vs. time for $\rho = 0, 2$ and $4m$ and parameter values $a_1 = 10^{-1}m$ and $a_2 = 10m$.

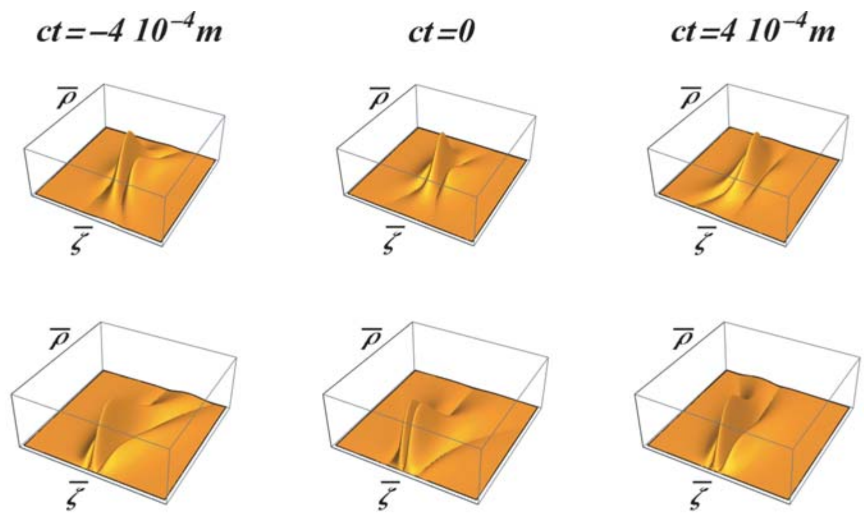

Figure 2. $|E_x|$ (top row) and $|E_z|$ (lower row) vs. $\bar{\varsigma} = \varsigma/a_1$ and $\bar{\rho} = \rho/(10a_1)$ for the parameter values $a_1 = 10^{-6}m$, $a_2 = 10^{-3}m$ and $n = 1$.

Figure 4 shows stream plots of the x and y components of the electromagnetic momentum (top row) and electromagnetic angular momentum (lower row) vs. x and y for $\tau = 0$ and $\tau = \pm 10s$ for the parameter values $a_1 = 10^{-2}m,\ a_2 = 10\,\mathrm{m}$ and $n = 1$.

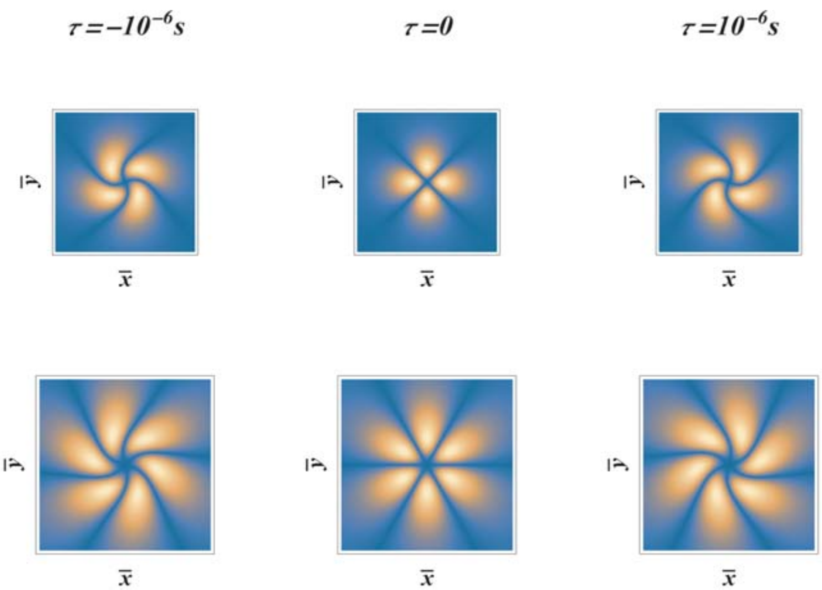

Figure 3. $|E_x|$ (top row) and $|E_z|$ (lower row) vs. $\bar{x} = x/(10^2 a_1)$ and $\bar{y} = y/(10^2 a_1)$ at $\tau = -10^{-6}s,\ 0$ and $10^{-6}s$ for the parameter values $a_1 = 10^{-6}m,\ a_2 = 10^{-3}m$ and $n = 3$.

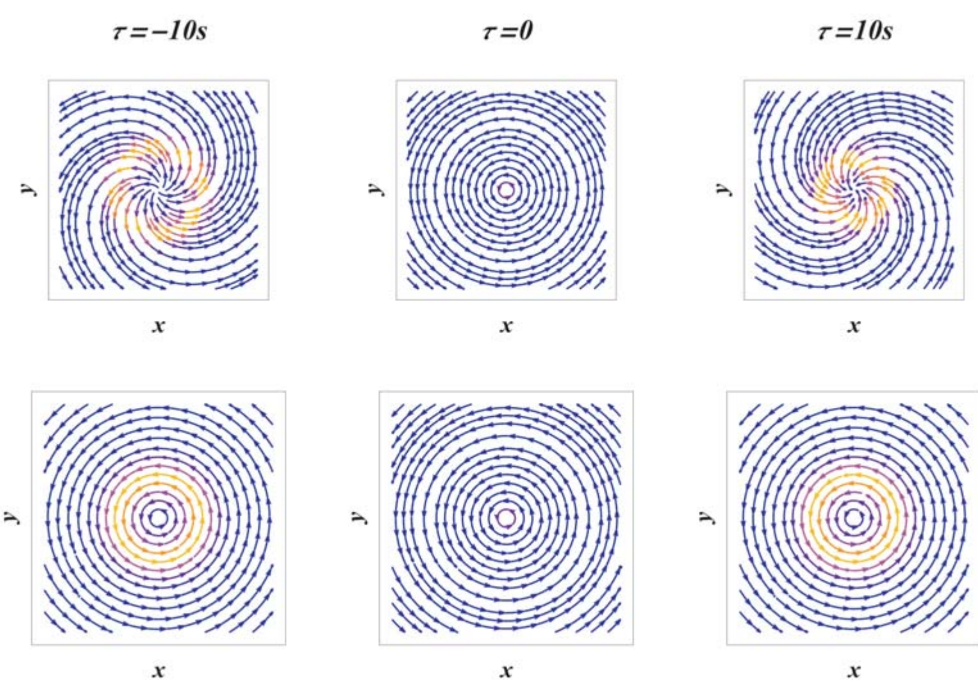

Figure 4. Stream plots of the x and y components of the electromagnetic momentum (upper row) vs. x and y at $\tau = -10s,\ 0$ and $10s$ for the parameter values $a_1 = 10^{-2}m,\ a_2 = 10m$ and $n = 1$. Similar plotsare shown on the second row for the electromagnetic angular momentum.

6. TOPOLOGICAL STRUCTURES OF ELECTROMAGNETIC WAVES

Irvine and Bouwmeester [11] explored the physical properties of an exceptional solution to the free-space Maxwell's equations *in vacuo* that exhibit linked and knotted field line structures. The Irvine-Bouwmeester solution was constructed originally by Ranãda [12] using Hopf maps (*fibrations*) and belongs to a more general class of solutions to linear and nonlinear equations known as *Hopfions*. Besieris and Shaarawi [13] have linked the Irvine-Bouwmeester solution to a known null luminal electromagnetic wave. This work has been further extended by Kedia *et al.* [14] and Arrayás *et al.* [15].

Consider the variation of the luminal Bateman conjugate functions

$$\begin{aligned} \alpha &= 1 + \left.\frac{2}{\alpha_L}\right|_{a_{1.2}=-1} = \frac{x^2+y^2+(z+i)^2-c^2t^2}{x^2+y^2+z^2-(ct-i)^2}, \\ \beta &= 2\left.\frac{\beta_L}{\alpha_L}\right|_{a_{1.2}=-1} = \frac{2(x-iy)}{x^2+y^2+z^2-(ct-i)^2} \end{aligned} \tag{16}$$

used in Ref. [14]. They have the property $\alpha\alpha^* + \beta\beta^* = 1$. The surface $|\alpha^2 - \beta^2| = \text{const.}$ represents two linked tori, $|\alpha^2 - \beta^3| = \text{const.}$ represents a trefoil knot, and $|\alpha^2 - \beta^5| = \text{const.}$ depicts a cinquefoil, for any value of time (see Fig. 5).

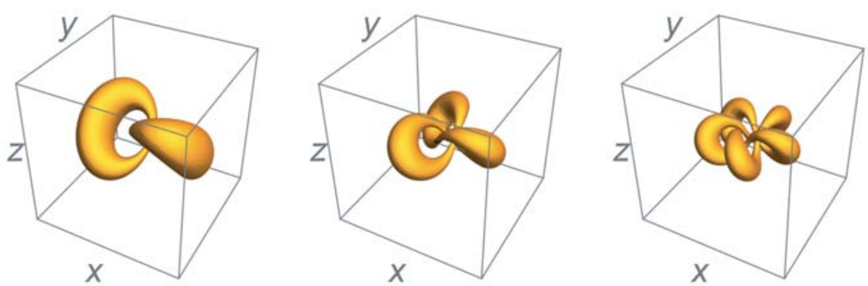

Figure 5. Plots of $|\alpha^p - \beta^q| = \text{const.}$ for $p = q = 2$ (torus link), $p = 2,\ q = 3$ (trefoil) and $p = 2,\ q = 5$ (cinquefoil).

When the expressions for the Bateman conjugate functions given in Eq. (16) are used in Eq. (7), the case $p = 1$ and $q = 1$, corresponding to the Hopf-Ranãda solution, yields linked electromagnetic fields. Any two electric field lines are linked, any two magnetic field lines linked, and any electric field line is linked to any magnetic field line for any instant of time. For $p = 2,\ q = 3$ and $p = 2,\ q = 5$ the linkages are more complicated (see Fig. 6). The corresponding fields have finite energy.

A negative aspect of the Hopf-Ranãda solution is that the Bateman conjugate functions in Eq. (16) contain equally weighted forward and backward components associated with the characteristic variables $z \pm ct$. On the other hand, physically realizable localized waves have free parameters that can be tweaked so that the wave packets have finite energy and propagate primarily along the z-direction. There exist Bateman-type conjugate functions that lead to such types of null electromagnetic waves and also are endowed with topological features similar to those of the Hopf-Ranãda solution. A particular example is provided by the Bateman conjugate functions

$$\begin{aligned} \alpha &= \frac{1}{\alpha_L^2} = \left(a_2 - i(z+ct) + \frac{x^2+y^2}{a_1 + i(z-ct)}\right)^2, \\ \beta &= \beta_L|_{y\to-y} = \frac{x+iy}{a_1+i(z-ct)} \end{aligned} \tag{17}$$

The change in sign of y in the definition of β will result in a change in the sign on the right-hand side of the first part of Eq. (2) and also, on the right-hand side of the Bateman constraint in Eq. (6). Due to the presence of the positive free parameters $a_{1,2}$, the Bateman conjugate functions no longer obey

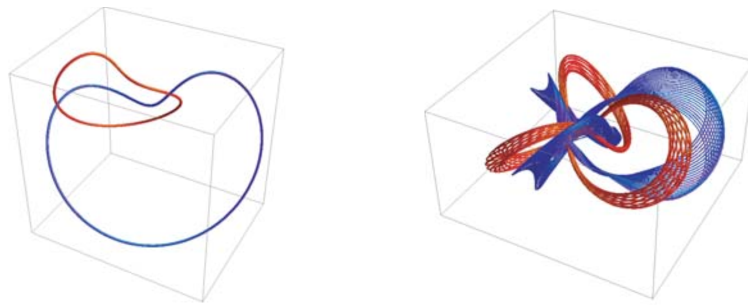

(a) (b)

Figure 6. EB field line linkages for (a) $p = q = 1$ and (b) $p = 2,\ q = 3$.

the relationship $\alpha\alpha^* + \beta\beta^* = 1$. For $p = 1$ and $q = 1$, the resulting null electromagnetic fields have all the topological linkage and knotted properties characterizing the Hopf-Ranãda solution. The main difference is that for $a_1 \ll a_2$ the wave has primarily forward propagating components. Another set of conjugate functions yielding a null spatiotemporally localized electromagnetic field having properties similar to those arising from the set in Eq. (17) is provided by a complexified version of functions derived by Hogan [16]; specifically,

$$\begin{aligned} \alpha &= -\frac{\left(b - AQ(x-iy) + BQ\left(a_2 - i(z+ct)\right)\right)^2}{\left(b\left(a_1 + (z-ct)\right) + BQ\left(x^2+y^2+\left(a_1+i(z-ct)\right)\left(a_2-i(z+ct)\right)\right)\right)^2}, \\ \beta &= x + iy - \frac{Q\left(a_2 - i(z+ct)\right)\left(B(x+iy) + A\left(a_1 + i(z-ct)\right)\right)}{b - AQ(x-iy) + iBQ\left(a_2 - i(z+ct)\right)}, \end{aligned} \tag{18}$$

where $a_{1,2},\ b,\ A,\ B$, and Q are free parameters. As in the case of the Bateman conjugate functions in Eq. (17), the critical parameters required for the reduction of the backward propagating waves are a_1 and a_2.

7. CONCLUDING REMARKS

Due to the complexity of $\psi(\vec{r}, t)$ in Eq. (4) and the ensuing spatiotemporal differentiations, the resulting real electromagnetic fields are, in general, quite complicated, and questions regarding total energy, momentum, and angular momentum content become nontrivial. Some of this complexity is alleviated in the case of null electromagnetic localized waves because the Riemann-Silberstein complex vector associated with such structures is given by

$$\vec{F}\left(\vec{r}, t\right) = \vec{F}^{(f)}\left(\vec{r}, t\right)\psi\left(\vec{r}, t\right)g^{-1}\left(\vec{r}, t\right), \tag{19}$$

in terms of the fundamental Riemann-Silberstein complex null vector, an arbitrary scalar localized wave obeying the Courant-Hilbert *ansatz*, and the corresponding attenuation function. In these cases, the structures of $\vec{F}(\vec{r}, t)$ and the corresponding real electric and magnetic fields $\vec{E}(\vec{r}, t)$ and $\vec{H}(\vec{r}, t)$ are simpler, thus facilitating the explicit computation of the total energy and angular momentum they carry.

It has been mentioned that null electromagnetic waves can be derived using the variation of the Hertz potential approach in Eq. (4). It turns out that the Hertz vector potential $\vec{\Pi}(\vec{r}, t) = \{i, 0, 0\}\psi_L(\vec{r}, t)$, with $\psi_L(\vec{r}, t)$ any scalar spatiotemporally localized luminal wave solution constructed according to Eq. (10), can result in such a solution. A specific example is the basic Hopfion that can be derived using the scalar wave solution

$$\psi_L\left(\vec{r}, t\right) = \frac{g_L}{a_L} = \frac{1}{a_1 + i\left(z - ct\right)}\left(a_2 - i\left(z + ct\right) + \frac{x^2 + y^2}{a_1 + i\left(z - ct\right)}\right)^{-1}, \tag{20}$$

with $a_{1,2} = 0$, and $t \to t - i/c$.

There exist classes of scalar localized waves which do not conform to the templates based on the Courant-Hilbert progressive wave theory discussed in Section 3. Interestingly, some of the localized waves belonging to these classes arise from the superposition of elementary Courant-Hilbert progressive LWs. A particular example is the Bessel-Gauss FWM

$$\psi_L^{(BG)}(\vec{r},t) = \frac{1}{a_1 + i(z-ct)} \exp\left[-k\alpha_L(\vec{r},t)\right] \exp\left[-\frac{p^2}{4k}\frac{1}{a_1+i(z-ct)}\right] I_0\left[p\frac{\sqrt{x^2+y^2}}{a_1+i(z-ct)}\right], \quad (21)$$

which can be derived by an integration of weighted FWMs. In this expression, k and p are positive free parameters with units of m^{-1}, and $I_0(\cdot)$ is the zero-order modified Bessel function. For $p = 0$, $\psi_L^{BG}(\vec{r},t)$ reduces to the FWM. The general theory of luminal null electromagnetic localized waves does not apply to the Bessel-Gauss FWM. In other words, although $\vec{F}_L = \vec{F}_L^{(f)}(\vec{r},t)\psi_L^{(BG)}(\vec{r},t)g_L^{-1}(\vec{r},t)$ is a null vector, it is not a Riemann-Silberstein complex vector. Specifically, it does not obey the expressions in Eq. (2). The reason for this is that $\psi_L^{(BG)}(\vec{r},t)g_L^{-1}(\vec{r},t)$ is not a pure functional of $\alpha_L(\vec{r},t)$, but it has an additional dependence on space and time, as it is clearly seen in Eq. (21). It should be pointed out, however, that it is possible to derive null Bessel-Gauss and other complicated spatiotemporally localized luminal electromagnetic waves by other means. Useful toward this goal are two vector-valued conformal techniques due to Cunningham [17] and Bateman [18] (See [9] for specific applications).

All the null electromagnetic localized waves discussed in this article are solutions to the homogeneous Maxwell equations in vacuum. An important question concerns their physical realizability. It is known that very close replicas of subluminal, luminal, and superluminal localized waves can be launched from apertures constructed on the basis of the Huygens principle [19]. All experimental demonstrations have been performed in the acoustical and optical regimes [20–28]. Work, however, has been carried out at microwave frequencies recently [29–32]. Null localized electromagnetic waves constitute a broad subset of ordinary spatiotemporally localized waves. Therefore, the experimental techniques used to physically realize the latter should also be applicable to the former. It would be very interesting, for example, to demonstrate experimentally a close replica of the basic Hopf-Ranãda (basic Hopfion) and examine whether its features pertaining to the linked and knotted topological properties of the electric and magnetic field lines can be exhibited.

REFERENCES

1. Weber, H., "Die partiellen Differential-Gleichungen der mathematischen Physik nach Riemann's Vorlesungen," Friedrich Vieweg und Sohn, Brunschweig, 1901.
2. Silberstein, L., "Electromagnetische Grundgleichungen in bivectorieller Behandlung," *Ann. D. Phys.*, Vol. 22, 579–586, 1907.
3. Bialynicki-Birula, I. and Z. Bialynicki-Birula, "The role of the Riemann-Silberstein vector in classical and quantum theories of electromagnetism," *J. Phys. A: Math. Theor.*, Vol. 46, 053001, 2013.
4. Whittaker, E. T., "On the expressions of the electromagnetic field due to electrons by means of two scalar potential functions," *Proc. London Math. Soc.*, Vol. 1, 367–372, 1904.
5. Bateman, H., *The Mathematical Analysis of Electrical and Optical Wave-Motion on the Basis of Maxwell's Equations*, Dover, New York, 1955.
6. Besieris, I. M., M. Abdel-Rahman, A. M. Shaarawi, and A. Chatzipetros, "Two fundamental representations of localized pulse solutions to the scalar wave equation," *Progress In Electromagnetics Research*, Vol. 19, 1–48, 1998.
7. Ziolkowski, R. W., "Exact solutions of the wave equation with complex sources," *J. Math. Phys.*, Vol. 26, 861–863, 1985.
8. So, I. A., A. B. Plachenov, and A. P. Kiselev, "Simple unidirectional finite-energy pulses," *Phys. Rev. A*, Vol. 02, 063529, 2020.
9. Besieris, I. M. and A. M. Shaarawi, "Spatiotemporally localized null electromagnetic waves I. Luminal," *Progress In Electromagnetics Research B*, Vol. 8, 1–28, 2008.

10. Besieris, I. M. and A. M. Shaarawi, "Spatiotemporally localized null electromagnetic waves," *Non-Diffracting Waves*, H. Hernandez-Figueroa, M. Zamboni-Rached, and E. Recami, ed., 161–188, Wiley, New York, 2013.
11. Irvine, W. T. M. and D. Bouwmeester, "Linked and knotted beams of light," *Nat. Phys.*, Vol. 4, 716–720, 2008.
12. Ranãda, A. F., "Knotted solutions of Maxwell equations in vacuum," *J. Phys. A: Math. Gen.*, Vol. 23, L815–L820, 1990.
13. Besieris, I. M. and A. M. Shaarawi, "Hopf-Ranãda linked and knotted light beam solution viewed as a null electromagnetic field," *Opt. Lett.*, Vol. 34, 3887–3889, 2009.
14. Kedia, H., I. Bialynicki-Birula, D. Peralta-Salas, and W. T. M. Irvine, "Tying knots in light fields," *Phys. Rev. Lett.*, Vol. 111, 150404, 2017.
15. Arrayás, M., D. Bouwmeester, and J. L. Trueba, "Knots in electromagnetism," *Phys. Rep.*, Vol. 667, 1–61, 2017.
16. Hogan, P. A., "Bateman electromagnetic waves," *Proc. R. Soc. Lond. A*, Vol. 396, 199–204, 1984.
17. Cunningham, E., "The principle of relativity in electrodynamics and an extension thereof," *Proc. London. Math. Soc.* Vol. 8, 77–98, 1909.
18. Bateman, H., "The transformation of electrodynamical equations," *Proc. London. Math. Soc.*, Vol. 8, 223–264, 1910.
19. Ziolkowski, R. W., A. M. Shaarawi, and I. M. Besieris, "Aperture realizations of the exact solutions to homogeneous-wave equations," *J. Opt. Soc. Am. A*, Vol. 10, 75–87, 1993.
20. Lu, J.-Y. and J. F. Greenleaf, "Experimental verification of nondiffracting X waves," *IEEE Trans. Ultrasonic. Ferroelec., Freq. Contr.*, Vol. 39, 441–446, 1992.
21. Saari, P. and K. Reivelt, "Evidence of X-shaped propagation-invariant localized light waves," *Phys. Rev. Lett.*, Vol. 79, 4135–4137, 1997.
22. Reivelt, K. and P. Saari, "Experimental demonstration of realizability of optical focus wave modes," *Phys. Rev. E*, Vol. 66, 056611-1-9, 2002.
23. Grunwald R., V. Kebbel, U. Griebner, U. Neumann, A. Kummrow, M. Rini, E. T. J. Nibbering, M. Piché, G. Rousseau, and M. Fortin, "Generation and characterization of spatially and temporally localized few-cycle optical wave packets," *Phys. Rev. A*, Vol. 67, 063820, 2003.
24. Bowlan, P., H. Valtna-Lukner, M. Lõhmus, P. Piksarv, P. Saari, and R. Trebino, "Measurement of the spatio-temporal field of ultrashort Bessel-X pulses," *Opt. Lett.*, Vol. 34, 2276, 2009.
25. Saari, P., "X-type waves in ultrafast optics," *Non-Diffracting Waves*, H. E. Hernandez-Figueroa, E. Recami, and M. Zamboni-Rached, ed., 109–134, Wiley, New York, 2013.
26. Kondakci, H. E. and A. F. Abouraddy, "Diffraction-free space-time light sheets," *Nat. Photon.*, Vol. 11, 733–740, 2017.
27. Bhaduri, B., M. Yessenov, and A. F. Abouraddy, "Space-time wave packets that travel in optical materials at the speed of light in vacuum," *Optica*, Vol. 6, 139–145, 2019.
28. Yessenov, M., B. Bhaduri, H. E. Kondakci, and A. F. Abouraddy, "Classification of propagation-invariant of space-time wave packets in free space," *Phys. Rev. A*, Vol. 99, 023856, 2019.
29. Mugnai D., A. Ranfagni, and R. Ruggeri, "Observation of superluminal behaviors in wave propagation," *Phys. Rev. Lett.*, Vol. 84, 4830, 2000.
30. Papasimakis, N., T. Raybould, V. A. Fedotov, D. P. Tsai, I. Youngs, and N. I. Zheludev, "Pulse generation scheme for flying electromagnetic doughnuts," *Phys. Rev. B*, Vol. 97, 201409-1-6, 2018.
31. Comite, D., W. Fuscaldo, S. K. Podilchak, and V. Gómez-Guillamón Buenndia, "Microwave generation of X-waves by means of planar leaky-wave antenna," *Appl. Phys. Lett.*, Vol. 113, 144102-1-5, 2018.
32. Fuscaldo, W., D. Comite, A. Boesso, P. Baccarelli, P. Bughignoli, and A. Galli, "Focusing leaky waves: A class of electromagnetic localized waves with complex spectra," *Phys. Rev. Appl.*, Vol. 9, 054005-1-15, 2018.